The function of heme-regulated eIF2α kinase in murine iron homeostasis and macrophage maturation

Sijin Liu, … , Nancy C. Andrews, Jane-Jane Chen

Research Article   Hematology

Heme-regulated eIF2α kinase (HRI) plays an essential protective role in anemias of iron deficiency, erythroid protoporphyria, and β-thalassemia. In this study, we report that HRI protein is present in murine macrophages, albeit at a lower level than in erythroid precursors. *Hri⁻/⁻* mice exhibited impaired macrophage maturation and a weaker antiinflammatory response with reduced cytokine production upon LPS challenge. The level of production of hepcidin, an important player in the pathogenesis of the anemia of inflammation, was significantly decreased in *Hri⁻/⁻* mice, accompanied by decreased splenic macrophage iron content and increased serum iron content. Hepcidin expression was also significantly lower, with a concomitant increase in serum iron in *Hri⁻/⁻* mice upon LPS treatment. We also demonstrated an impairment of erythrophagocytosis by *Hri⁻/⁻* macrophages both in vitro and in vivo under chronic hemolytic anemia, providing evidence for the role of HRI in recycling iron from senescent red blood cells. This work demonstrates that HRI deficiency attenuates hepcidin expression and iron homeostasis in mice, indicating a potential role for HRI in the anemia of inflammation.

Find the latest version:

The function of heme-regulated eIF2α kinase in murine iron homeostasis and macrophage maturation

Sijin Liu,[1] Rajasekhar N.V.S. Suragani,[1] Fudi Wang,[2] Anping Han,[1] Wanting Zhao,[1] Nancy C. Andrews,[2] and Jane-Jane Chen[1]

[1]Harvard-MIT Division of Health Sciences and Technology, Massachusetts Institute of Technology, Cambridge, Massachusetts, USA.
[2]Division of Hematology/Oncology, Children's Hospital Boston and Harvard Medical School, Boston, Massachusetts, USA.

Heme-regulated eIF2α kinase (HRI) plays an essential protective role in anemias of iron deficiency, erythroid protoporphyria, and β-thalassemia. In this study, we report that HRI protein is present in murine macrophages, albeit at a lower level than in erythroid precursors. *Hri⁻/⁻* mice exhibited impaired macrophage maturation and a weaker antiinflammatory response with reduced cytokine production upon LPS challenge. The level of production of hepcidin, an important player in the pathogenesis of the anemia of inflammation, was significantly decreased in *Hri⁻/⁻* mice, accompanied by decreased splenic macrophage iron content and increased serum iron content. Hepcidin expression was also significantly lower, with a concomitant increase in serum iron in *Hri⁻/⁻* mice upon LPS treatment. We also demonstrated an impairment of erythrophagocytosis by *Hri⁻/⁻* macrophages both in vitro and in vivo under chronic hemolytic anemia, providing evidence for the role of HRI in recycling iron from senescent red blood cells. This work demonstrates that HRI deficiency attenuates hepcidin expression and iron homeostasis in mice, indicating a potential role for HRI in the anemia of inflammation.

Introduction

Systemic iron homeostasis is strictly regulated to supply the appropriate amount of iron for growth and survival while preventing either iron deficiency or iron excess (reviewed in refs. 1, 2). Iron deficiency anemia is one of the most prevalent human diseases and has long been known to impair physical and mental function (3). On the other hand, iron overload is also deleterious (2, 4, 5). Although the molecular mechanisms of this strictly regulated iron homeostasis remain to be fully elucidated, the liver-produced hormone hepcidin seems to be the key regulator (reviewed in refs. 1, 2). Disruption of hepcidin gene expression in mice (6, 7) and humans (8) resulted in iron overload, while overexpression of hepcidin in mice caused severe iron deficiency anemia (9). Hepcidin controls plasma iron levels by inhibiting the absorption of dietary iron from the intestine and the release of iron from senescent rbc by macrophages (reviewed in refs. 1, 2). Hepcidin exerts this function by binding to the iron exporter ferroportin and targeting ferroportin for degradation (10). Hepcidin expression is homeostatically regulated by body iron status, inflammation, and erythropoietic needs. It is enhanced by iron overload (11) and inflammation (12–15) and is inhibited by anemia and hypoxia (12). Recently, it has been shown that repression of hepcidin production in anemia and by erythropoietin requires erythropoietic activity (16, 17). These different means of the regulation of hepcidin allow it to limit intestinal absorption during iron overload and to increase iron availability when needed for erythropoiesis.
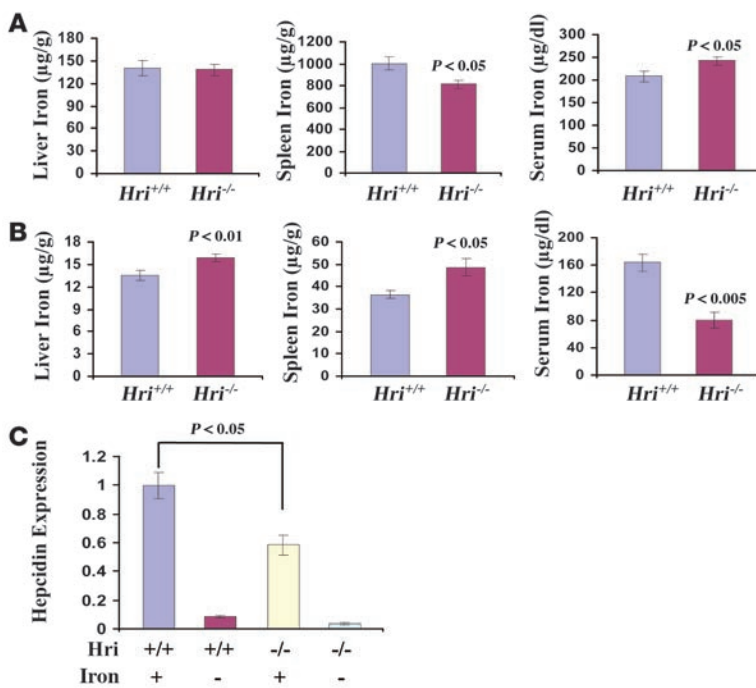
The discovery that hepcidin expression is directly regulated by inflammatory cytokines has linked hepcidin to anemia of inflammation (AI), also known as anemia of chronic disease and hypoferremia of inflammation (refs. 18, 19, and reviewed in refs. 20, 21). AI has been recognized for more than a century (22). It is commonly observed in patients with chronic diseases and is associated with decreased serum iron and iron-laden bone marrow macrophages (23). This sequestration of iron is thought to starve invading microbes and cancer cells of iron, which is necessary for cell proliferation. It has been shown that increased hepcidin production in a patient with benign liver tumor resulted in iron-refractory anemia, which disappeared after removal of the tumor (24). Furthermore, urinary hepcidin levels were elevated in patients with infections and inflammatory diseases (13).

To date, our laboratory has demonstrated that heme-regulated eIF2α kinase (HRI) is expressed mainly in erythroid cells and is an important physiological regulator of gene expression and cell survival in the erythroid lineage. HRI plays essential protective roles in iron deficiency (25), erythropoietic protoporphyria (EPP), and β-thalassemia (26). HRI exerts these functions in part by controlling protein synthesis via phosphorylation of the α-subunit of the eukaryotic translational initiation factor 2 (eIF2α). HRI is regulated by heme through 2 heme-binding domains in the N terminus and the kinase insertion (KI) domain. In heme deficiency, heme dissociates from the binding site in the KI domain and HRI is activated. Thereafter, eIF2α is phosphorylated, which inhibits the recycling of eIF2 for another round of protein synthesis (reviewed in ref. 27). Thus, HRI normally insures that no globin is synthesized in excess of what can be assembled into hemoglobin tetramers, which is dependent on the amount of heme available. In the absence of HRI and under conditions of iron deficiency, free globins precipitate within rbc and their precursors, resulting in hyperchromic, normocytic anemia with decreased rbc counts and

Figure 1
Effects of HRI and iron deficiencies on tissue iron, serum iron, and hepatic hepcidin expression. (**A**) Hepatic, splenic, and serum iron content in *Hri*^{+/+} and *Hri*^{–/–} mice. (**B**) Hepatic, splenic, and serum iron contents in iron-deficient *Hri*^{+/+} and *Hri*^{–/–} mice. (**C**) Hepatic hepcidin mRNA in *Hri*^{+/+} and *Hri*^{–/–} mice during iron deficiency. Hepcidin expression was significantly decreased in iron deficiency ($P < 0.01$, compared with respective control mice). Hepcidin expression was also significantly decreased in *Hri*^{–/–} mice ($P < 0.05$ for both iron-sufficient and iron-deficient conditions). Serum and tissue samples were collected from 4-month-old mice. Hepcidin mRNA was analyzed by qRT-PCR and normalized with eIF2α. Hepcidin expression in *Hri*^{+/+} was defined as 1. Results are presented as mean ± SEM (n = 6–9).

adding a major cell destruction component to the pathophysiology of the anemia. In addition, HRI is required for the survival of erythroid precursors in iron deficiency (25). HRI is also activated by non-heme cytoplasmic stresses such as oxidative stress and heat shock (28) and is activated in β-thalassemia to reduce the severity of the disease (26).

Since HRI plays such an important role in the production of hemoglobin and formation of the rbc that contain nearly 70% of the total body iron, it may also play an important role in systemic and cellular iron homeostasis. We therefore investigated iron homeostasis and hepcidin expression in HRI deficiency. Here, we report the novel function of HRI in macrophages. Expression of HRI, albeit at a lower level than in erythroid precursors, is necessary for the maturation of macrophages, their capacity for erythrophagocytosis, and their inflammatory response to LPS. In addition, hepatic hepcidin mRNA levels are decreased in HRI deficiency both at the basal level and upon LPS treatment. We also observed the impairment of erythrophagocytosis by *Hri*^{–/–} macrophages and diminished iron recycling in *Hri*^{–/–} mice under chronic hemolytic anemia induced by phenylhydrazine (PHZ). This study demonstrates the function of HRI in iron homeostasis and indicates that HRI may also be important in AI and hemolytic anemia.

Results

Iron homeostasis and hepcidin expression in HRI deficiency. To investigate the role of HRI in iron homeostasis, we determined non-heme iron content in the liver, spleen, and serum of 4-month-old mice under both normal and iron-deficient conditions. The splenic iron was significantly reduced in *Hri*^{–/–} mice (18.8%; $P < 0.05$) compared with *Hri*^{+/+} mice. In addition, there was a corresponding increase in serum iron of *Hri*^{–/–} mice (16.5%; $P < 0.05$). However, the hepatic iron was not significantly changed (Figure 1A). It is important to note that non-heme iron in the spleen was mainly localized in the macrophages and the iron content in the macrophages was reduced in HRI deficiency.

In iron deficiency, *Hri*^{–/–} mice had more hepatic iron (17.9%; $P < 0.01$) and more splenic iron (33.4%; $P < 0.05$) than *Hri*^{+/+} mice but had less serum iron (50.9%; $P < 0.005$) than *Hri*^{+/+} mice (Figure 1B). This difference in iron homeostasis of *Hri*^{–/–} mice between iron-sufficient and -deficient conditions is likely to be a consequence of the ineffective erythropoiesis occurring in *Hri*^{–/–} mice under iron deficiency (25).

To elucidate the molecular mechanism for the decreased splenic iron content in *Hri*^{–/–} mice, we determined hepcidin expression in the liver. As shown by quantitative RT-PCR (qRT-PCR) analysis (Figure 1C), hepatic hepcidin mRNA was significantly reduced, by 41.0%, in *Hri*^{–/–} mice compared with *Hri*^{+/+} mice. This decreased hepcidin expression is consistent with the decreased splenic iron and increased serum iron in *Hri*^{–/–} mice. As expected, in iron deficiency, hepatic hepcidin expression was reduced by 91% in *Hri*^{+/+} mice. Hepcidin expression was also reduced by 96% in combined HRI and iron deficiencies (Figure 1C).

Expression of HRI in macrophages. To help understand how HRI might regulate iron content in splenic macrophage and hepatic hepcidin expression as described above, we examined the expression of HRI in bone marrow–derived macrophages (BMDMs) cultured in vitro with CSF-1. We found by qRT-PCR that expression of HRI mRNA in BMDMs was approximately 2% of that in fetal liver erythroid precursors (data not shown). Expression of HRI protein in BMDMs was also demonstrated by immunofluorescence microscopy (Figure 2A) and Western blot analysis (Figure 2B). Most HRI-positive cells were Mac-1–positive macrophages, and HRI protein was located in the cytoplasm of macrophages (Figure 2A). Consistent with qRT-PCR results, HRI protein in BMDMs was also expressed at a lower level than that in fetal liver erythroid precursors (Figure 2B).

We have shown previously that HRI is predominantly expressed in the erythroid lineage (29). This is the first demonstration to our knowledge that HRI protein is expressed at a substantial level in non-erythroid cells. Most significantly, the level of phosphorylated eIF2α (eIF2αP) in *Hri*^{–/–} BMDMs was diminished (about 50%) as compared
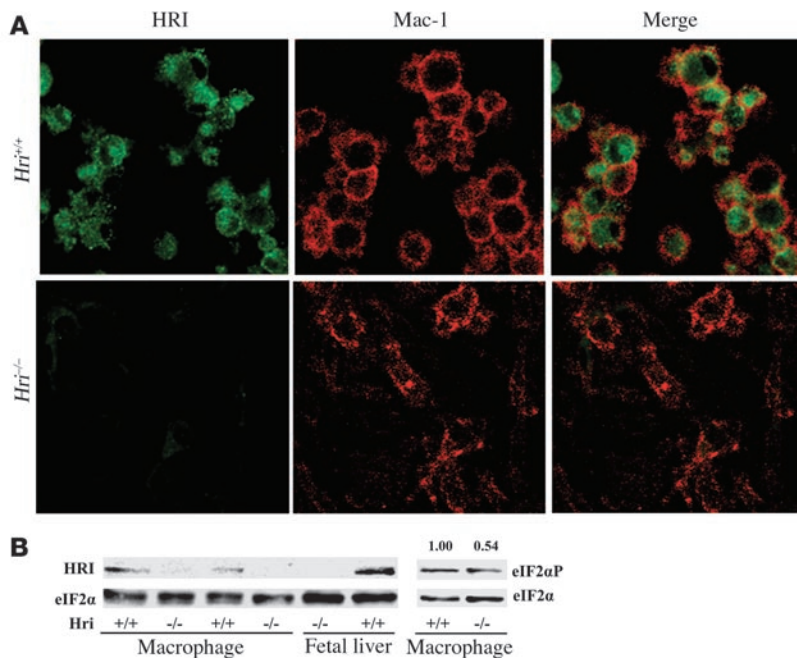
Figure 2
Expression of HRI protein in BMDMs. (**A**) Immuno-
fluorescence staining of HRI and Mac-1 in *Hri*+/+ and
Hri–/– macrophages. Original magnification, ×400. (**B**)
Western blot analyses of HRI protein, eIF2αP, and
total eIF2α levels in *Hri*+/+ and *Hri*–/– macrophages
and E14.5 fetal liver cells. The intensities of autora-
diograms were quantitated as described in Methods.
The ratios of eIF2αP to eIF2α were calculated; the
ratio in *Hri*+/+ was defined as 1. The normalized ratios
are shown above the autoradiogram.

with that in *Hri*+/+ BMDMs (Figure 2B). These results demonstrate that HRI is not only expressed in BMDMs but is also active and functional in phosphorylating its substrate, eIF2α. HRI contributes to 50% of the total eIF2α kinase activity in macrophages.

Impairment of macrophage maturation in HRI deficiency. As shown by phase-contrast microscopy, BMDMs began to mature and form outward protrusions at the peripheral membrane in *Hri*+/+ by day 3 of in vitro culture. In contrast, *Hri*–/– BMDMs were still round, without outward protrusions (Figure 3A). On day 6, most *Hri*+/+ cells were typical macrophages; however, *Hri*–/– BMDMs were still less mature, with fewer podosomes, as shown in Figure 3A.

In vivo, the expression of CD11b (Mac-1) macrophage surface marker was 9.82% less in *Hri*–/– bone marrow cells than in *Hri*+/+ bone marrow cells (day 0, $P < 0.05$; Figure 3B). After culturing bone marrow cells in vitro for 3 days with CSF-1, 96%–99% cells derived from both *Hri*+/+ and *Hri*–/– bone marrow were F4/80- and CD11b-positive, with a significant increase in the expression levels of both macrophage surface markers. However, the expression levels of both CD11b and F4/80 in *Hri*–/– BMDMs were still lower than those in *Hri*+/+ BMDMs on both day 3 and day 6 ($P < 0.05$; Figure 3B).

CSF-1 receptor (CSF-1R) is required for macrophage maturation and growth (reviewed in ref. 30). We found that CSF-1R protein was reduced by 20%–25% in *Hri*–/– BMDMs on both day 3 and day 6, as shown by Western blot analysis (Figure 3C). Collectively, these results demonstrate that *Hri*–/– BMDMs are impaired in their maturation and that decreased CSF-1R expression is likely to be responsible for the impaired maturation.
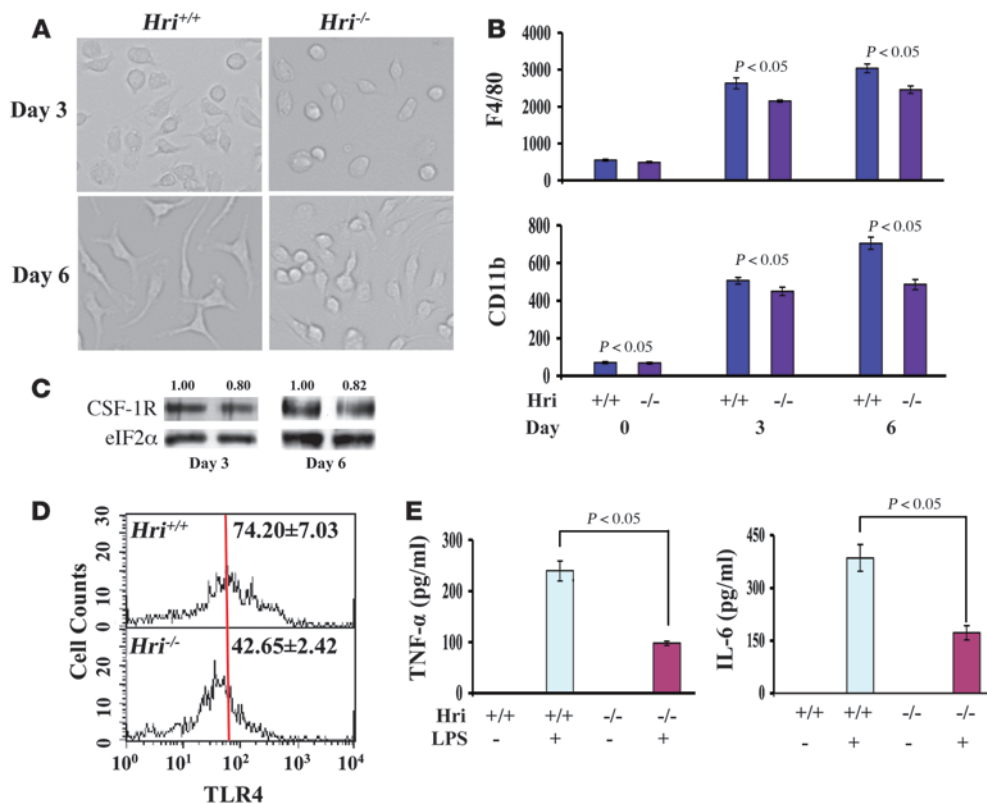
Blunted inflammatory response in HRI deficiency. As shown in Figure 3D, protein expression of TLR4, which plays an important role in sensing LPS, was decreased by 42.5% ($P < 0.005$) in *Hri*–/– macrophages by FACS analysis. We then examined the effect of HRI deficiency on the inflammatory response of macrophages. Both *Hri*+/+ and *Hri*–/– mice and their BMDMs cultured in vitro were treated with LPS. We measured levels of inflammatory cytokines IL-1β, IL-6, and TNF-α in culture media of BMDMs and in mouse sera. The levels of TNF-α, IL-1β, and IL-6 were below the limit of detection

in the culture media of both *Hri*+/+ and *Hri*–/– BMDMs prior to LPS treatment. After 6 hours of LPS treatment, TNF-α and IL-6 levels in the culture media were substantially increased in both *Hri*+/+ and *Hri*–/– BMDMs (Figure 3E). However, the response to LPS treatment was weaker in *Hri*–/– compared with *Hri*+/+ BMDMs; levels of TNF-α and IL-6 produced by *Hri*–/– BMDMs were about 50% of those in *Hri*+/+ BMDMs (Figure 3E; $P < 0.05$). IL-1β levels in both *Hri*+/+ and *Hri*–/– macrophage culture media were below the limit of detection even after 6 hours of LPS treatment (data not shown).

In vivo, serum IL-6 was greatly increased after 6 hours of treatment with LPS. However, the increase in IL-6 in *Hri*+/+ mice (100-fold) was greater than that in *Hri*–/– mice (50-fold) (Figure 4A). Similarly, TNF-α was increased 2.4-fold in *Hri*+/+ but only 1.8-fold in *Hri*–/– mice (Figure 4B). IL-1β was increased 4.3-fold in *Hri*+/+ versus 3.3-fold in *Hri*–/– mice (Figure 4C). The weaker inflammatory response of *Hri*–/– macrophages and *Hri*–/– mice to LPS is consistent with decreased TLR4 expression in *Hri*–/– macrophages (Figure 3D). These results indicate that expression of HRI in macrophages is required for the full LPS-induced acute inflammatory response both in vitro and in vivo.

Acute inflammation is known to induce hepcidin expression (reviewed in refs. 1, 2). As shown in Figure 4D, the increase in hepcidin following LPS treatment was greater in *Hri*+/+ (2.1-fold) than in *Hri*–/– mice (1.4-fold). Furthermore, the hepcidin level in *Hri*–/– mice after LPS treatment was still lower than that in *Hri*+/+ mice without LPS treatment (Figure 4D). This lower hepcidin level in *Hri*–/– mice upon LPS challenge correlated with lower inflammatory cytokine production (particularly IL-6) under these conditions.

To examine the effect of loss of HRI on hypoferremia upon LPS treatment, non-heme iron concentrations in sera, spleen, and liver of *Hri*+/+ and *Hri*–/– mice were measured. No significant changes in these parameters were observed in either *Hri*+/+ or *Hri*–/– mice at 6 hours after LPS treatment (data not shown). But at 24 hours after LPS treatment, serum iron concentrations in *Hri*+/+ mice were significantly decreased, from 206 μg/dl to 75 μg/dl (63.6%; Figure 4E), similar to previous reports (31). Serum iron concentrations

Figure 3
Impairment of macrophage maturation and LPS response in $Hri^{-/-}$ BMDMs. (**A**) Cell morphology of $Hri^{+/+}$ and $Hri^{-/-}$ BMDM cultures. Phase-contrast images of BMDMs at days 3 and 6; original magnification, ×200. (**B**) FACS analyses of expression of macrophage surface markers F4/80 and CD11b. The y axes shows peak intensity (AU). (**C**) Western blot analyses of CSF-1R protein expression at days 3 and 6. The ratios of CSF-1R to eIF2α are shown above the autoradiogram. (**D**) FACS analyses of TLR4 protein expression at day 6. The peak intensity is shown in the upper-right corner of each diagram ($P < 0.01$). (**E**) Production of TNF-α and IL-6 upon LPS treatment. TNF-α and IL-6 in the culture media were measured by ELISA. Bone marrow macrophages from 6- to 8-week-old male mice were cultured, and results are presented as mean ± SEM (n = 3–4).

in $Hri^{-/-}$ mice were also significantly decreased, from 244 μg/dl to 127 μg/dl (47.9%; Figure 4E), but to a lesser extent than that in $Hri^{+/+}$ mice ($P < 0.01$). Concomitantly, splenic iron concentrations in both $Hri^{+/+}$ and $Hri^{-/-}$ mice were significantly increased (Figure 4E). However, the splenic iron of LPS-treated $Hri^{-/-}$ mice was still significantly less than that of $Hri^{+/+}$ mice ($P < 0.01$; Figure 4E). There was no significant change in liver non-heme iron concentration in either group of mice after treatment with LPS (Figure 4E). The differences in serum and splenic iron between $Hri^{+/+}$ and $Hri^{-/-}$ mice upon LPS treatment are consistent with the lower level of hepcidin in $Hri^{-/-}$ mice under these conditions (Figure 4D). Together, these results demonstrate that HRI is required for efficient sequestration of iron in the spleen and subsequent hypoferremia in serum upon acute inflammation induced by LPS.

Activation of HRI signaling pathway by LPS. To investigate the mechanism by which HRI sustained the inflammatory response by LPS treatment, activation of the HRI signaling pathway was examined. At the basal level, $Hri^{+/+}$ BMDMs had a higher levels of eIF2αP than $Hri^{-/-}$ BMDMs (Figures 2 and 5). Upon LPS treatment, eIF2αP levels increased from 0.5 to 6 hours in both $Hri^{+/+}$ and $Hri^{-/-}$ BMDMs. However, the level of eIF2αP in $Hri^{+/+}$ BMDMs was twice that in $Hri^{-/-}$ BMDMs at all time points examined (Figure 5A). In addition, we observed that HRI was hyperphosphorylated in $Hri^{+/+}$ BMDMs after LPS treatment, as shown by the upshift of HRI in SDS-PAGE at 3 and 6 hours (Figure 5A). These results show that HRI is activated in macrophages upon LPS treatment and leads to the increased level of eIF2αP. The increase in eIF2αP observed in $Hri^{-/-}$ BMDMs is likely due to the activation of another eIF2αP kinase, PKR (32).

LPS treatment was known to generate ROS (33). We reported earlier that ROS was involved in the activation of HRI by autophosphorylation upon arsenite stress in erythroid cells (28). We

therefore examined the activation of HRI in macrophages by ROS upon LPS treatments. After LPS treatment, the ROS level increased from 0.5 to 6 hours in both $Hri^{+/+}$ and $Hri^{-/-}$ macrophages as detected by the oxidation of 2′7′-dichlorodihyfluorosceine (DCF) (data not shown). As shown in Figure 5B, peaks of DCF fluorescence were shifted to a higher intensity in both $Hri^{+/+}$ and $Hri^{-/-}$ macrophages at 6 hours after LPS treatment. There was no significant difference between $Hri^{+/+}$ and $Hri^{-/-}$ macrophages in ROS production. Furthermore, this increase in ROS was prevented by β-mercaptoethanol (β-ME). β-ME had no effect on the level of ROS in control cells. Most importantly, LPS-enhanced eIF2αP in $Hri^{+/+}$ cells were also prevented by treatment with β-ME (Figure 5C). Together, these results demonstrate that activation of HRI by LPS in BMDMs is mediated by ROS.

One of the downstream events of the eIF2αP signal pathway is the induction of the transcriptional factor C/EBP homology protein (Chop) (34, 35). We found that at the basal level, Chop were also expressed at a higher level in $Hri^{+/+}$ than in $Hri^{-/-}$ BMDMs, consistent with increased eIF2αP in $Hri^{+/+}$ BMDMs. In addition, Chop expression was increased upon LPS treatment of $Hri^{+/+}$ BMDMs (Figure 5A), and this increase was prevented by treatment with β-ME (Figure 5C). Although Chop was also increased in response to LPS in $Hri^{-/-}$ BMDMs, its expression was delayed and occurred at a later time (Figure 5A). These observations demonstrate for the first time to our knowledge the activation of HRI signaling pathway upon LPS treatment in macrophages. This pathway may be important for the full production of inflammatory cytokines by macrophages upon challenge with LPS.

Reduced erythrophagocytosis in HRI deficiency. Since recycling of iron from senescent rbc by macrophages plays a critical role in iron homeostasis, we examined erythrophagocytosis of senescent
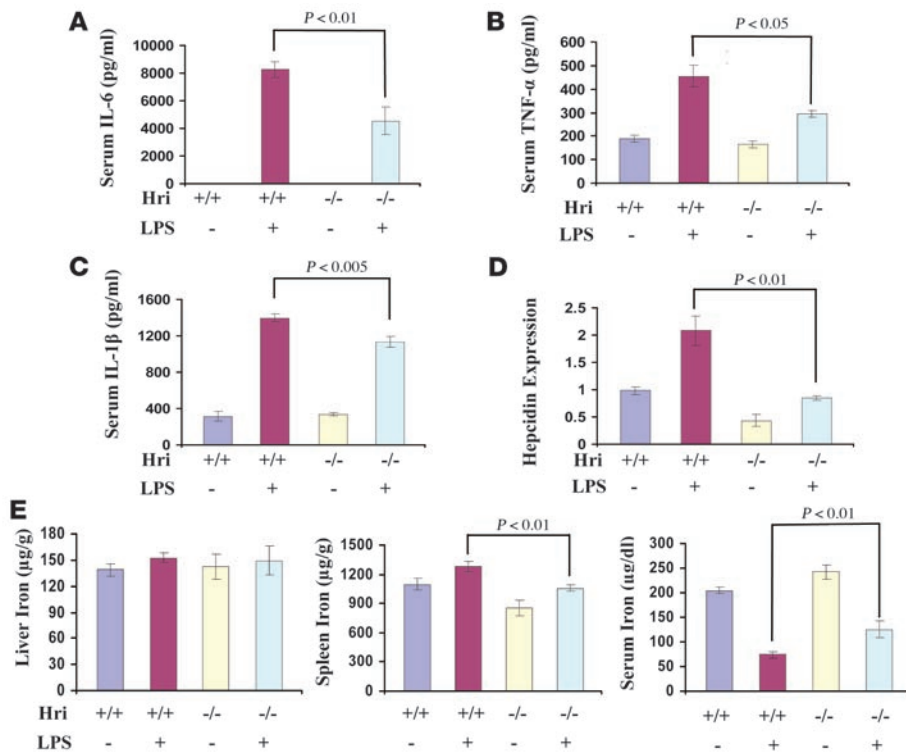
Figure 4
Impaired response to LPS treatment in *Hri*^{-/-} mice. Serum IL-6 (**A**), TNF-α (**B**), and IL-1β (**C**) levels of *Hri*^{+/+} and *Hri*^{-/-} mice at 6 hours after LPS treatment. (**D**) Hepatic hepcidin level in *Hri*^{+/+} and *Hri*^{-/-} mice at 6 hours after LPS treatment. (**E**) Hepatic, splenic, and serum iron content in *Hri*^{+/+} and *Hri*^{-/-} mice at 24 hours after LPS treatment. Hepatic iron content in *Hri*^{+/+} and *Hri*^{-/-} mice was not significantly changed after LPS treatment. Splenic iron content was significantly increased after LPS treatment in both *Hri*^{+/+} and *Hri*^{-/-} mice ($P < 0.05$); however, the splenic iron content after LPS treatment in *Hri*^{-/-} mice was significantly lower than that in *Hri*^{+/+} mice ($P < 0.01$). Serum iron was significantly decreased after LPS treatment in both *Hri*^{+/+} and *Hri*^{-/-} mice ($P < 0.001$); however, the serum iron in *Hri*^{-/-} mice was significantly higher than that in *Hri*^{+/+} mice after LPS treatment ($P < 0.01$). Four-month-old male mice were used, and hepcidin mRNA was analyzed as described in the legend of Figure 1. Hepcidin expression in *Hri*^{+/+} was defined as 1. Results are presented as mean ± SEM ($n = 6$–9).

rbc by *Hri*^{+/+} and *Hri*^{-/-} macrophages. Aging of rbc was simulated by increasing cellular calcium concentration. After treatment with calcium chloride and Ca^{2+} ionophore A23187, greater than 99% of rbc were positive for annexin V, while only 0.5% in untreated rbc were positive (data not shown). Only aged rbc were ingested by macrophages. As shown in Figure 6A, *Hri*^{+/+} macrophages engulfed more rbc than *Hri*^{-/-} macrophages both at baseline and upon treatment with LPS. The phagocytosis index (number of rbc/macrophage) was lower in untreated *Hri*^{-/-} macrophages and LPS-treated *Hri*^{-/-} macrophages (Figure 6B). Furthermore, the percentage of macrophages containing ingested rbc was also significantly lower in HRI deficiency (Figure 6B). These results demonstrate that there is an impairment of erythrophagocytosis by *Hri*^{-/-} macrophages resulting in a lower phagocytosis index and lower percentage of macrophages with ingested rbc.

Role of HRI in iron recycling during chronic hemolytic anemia. To investigate the role of HRI in erythrophagocytosis in vivo, we have examined erythrophagocytosis and iron homeostasis in a mouse model of chronic hemolytic anemia induced by treatment with a low dose of PHZ. After PHZ treatment, both *Hri*^{+/+} and *Hri*^{-/-} mice developed a very mild anemia with increased reticulocyte counts (31.85% in *Hri*^{+/+} and 53.29% in *Hri*^{-/-} mice; $P < 0.001$) and splenomegaly (6-fold enlargement) but no significant decrease in hemoglobin content compared with control mice. These results demonstrated that the PHZ-induced chronic hemolytic anemia was well compensated in both *Hri*^{+/+} and *Hri*^{-/-} mice.

The hepatic hepcidin mRNA level was greatly decreased in PHZ-treated *Hri*^{+/+} and *Hri*^{-/-} mice ($P < 0.001$), in agreement with increased erythropoiesis. However, the hepcidin level in *Hri*^{-/-} mice was lower than that in *Hri*^{+/+} mice both with and without PHZ treatment ($P < 0.05$) (Figure 7A). As previously reported (36, 37), both hepatic and splenic non-heme iron content were increased after

PHZ treatment (Figure 7B), consistent with the increased intestinal iron absorption in response to decreased hepcidin expression. However, these increases in iron content by PHZ treatment were significantly lower in *Hri*^{-/-} mice. The hepatic and splenic iron concentrations in *Hri*^{+/+} mice were 18.7% and 20.5% lower, respectively (Figure 7B). Interestingly, serum iron was decreased after PHZ treatment in both *Hri*^{+/+} and *Hri*^{-/-} mice (Figure 7B), even though hepcidin expression was decreased. This is most likely attributable to the increased erythropoietic iron utilization. The slight increase in serum iron in PHZ-treated *Hri*^{-/-} mice compared with PHZ-treated *Hri*^{+/+} mice ($P < 0.05$; Figure 7B) may have been due to increased iron export by higher amounts of ferroportin protein as the result of lower hepcidin level in PHZ-treated *Hri*^{-/-} mice (Figure 7A).

Importantly, non-heme iron staining of liver and spleen sections revealed that iron was present mainly in macrophages. Thus, the increase in non-heme iron in both spleen and liver were due to increased erythrophagocytosis of macrophages as the result of rbc damage by PHZ. As shown in Figure 8A, the difference in iron-laden macrophages between *Hri*^{+/+} and *Hri*^{-/-} mice was most prominent in the liver. There was no visible iron staining in control livers. Livers from PHZ-treated mice exhibited iron staining only in the Kupffer cells and not in hepatocytes. Furthermore, ingested rbc were visible in Kupffer cells (Figure 8A). We observed that PHZ-treated *Hri*^{-/-} livers had 35.5% fewer iron-laden Kupffer cells (38.4 cells/field compared with 59.5 cells/field in *Hri*^{+/+}) and less iron per macrophage as indicated by the intensity of iron staining (Figure 8B).

Together, these results demonstrate that increased iron in PHZ-induced hemolytic anemia is utilized entirely for erythropoiesis such that there is a decrease in serum iron and absence of iron accumulation in hepatocytes. Under this chronic hemolytic anemia condition, recycling of iron from senescent rbc plays an important role in providing iron for erythropoiesis, as evidenced
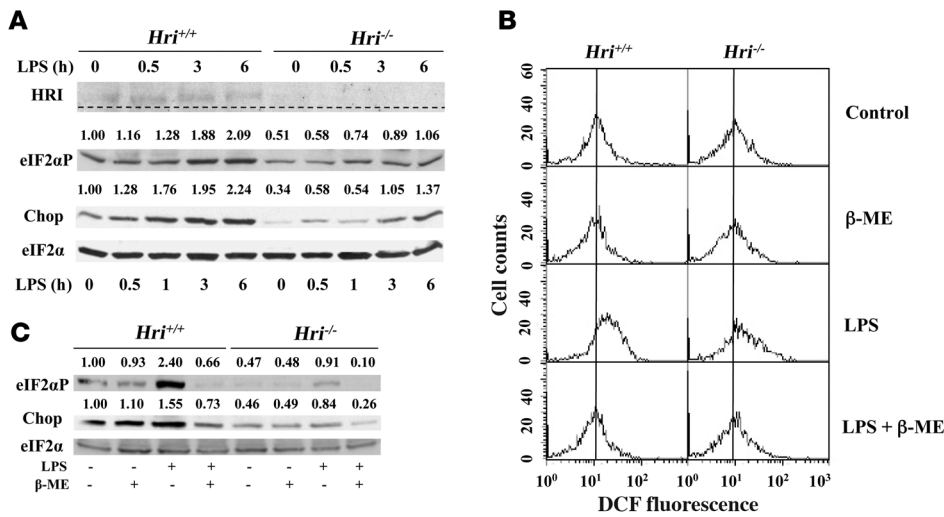
A

B

C

HRI exerts these functions by inhibition of translational initiation to reduce globin and heme synthesis under these disease conditions. This prominent role of HRI in rbc disorders is correlated with its higher level of expression in the erythroid lineage. However, the physiological function of HRI beyond erythroid cells is still unknown.
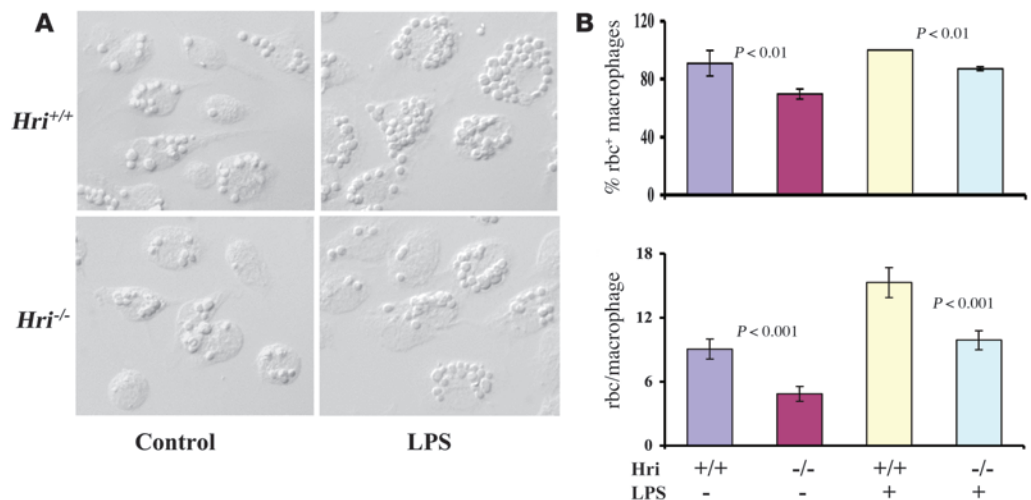
Macrophages are pivotal constituents of the innate immune system, vital for recognition and elimination of microbial pathogens (38). Macrophages are also responsible for iron recycling, taking iron from the hemoglobin of senescent rbc by phagocytosis and releasing it to the serum through ferroportin (reviewed in refs. 1, 2). We demonstrate here that HRI protein is expressed in macrophages (Figure 2). Although HRI is expressed at a lower level in macrophages, it is important for macrophage maturation. In HRI deficiency, macrophages did not develop the typical morphology and expressed less CSF-1R protein (Figure 3). CSF-

Figure 5
Activation of the HRI/eIF2αP pathway in BMDMs by LPS. (**A**) Time course of the activation of HRI signaling pathway upon LPS treatment. Cells were harvested after LPS treatment at the time points indicated, and equal amounts of protein extracts were analyzed for expression of HRI, eIF2αP, Chop, and total eIF2α by Western blot analyses. (**B**) ROS production in macrophages upon LPS treatment. DCF fluorescence in macrophages was measured by FACS analysis after 6-hour LPS treatment with or without β-ME (*n* = 3). (**C**) Prevention of the activation of HRI signaling pathway by LPS with β-ME. After 6-hour LPS treatment in the presence or absence of β-ME, expression of eIF2αP, Chop, and total eIF2α proteins was analyzed. The ratios of eIF2αP to eIF2α and Chop to eIF2α were calculated. The ratio of each at time 0 was defined as 1. The normalized ratios are shown above the autoradiograms.

by iron-laden Kupffer cells in the liver and macrophages in the spleen. Lower iron contents in hepatic and splenic macrophages of PHZ-treated *Hri⁻/⁻* mice compared with PHZ-treated *Hri⁺/⁺* mice indicate a decrease in erythrophagocytosis by *Hri⁻/⁻* macrophages in vivo. These results are consistent with the impairment of erythrophagocytosis in *Hri⁻/⁻* macrophages cultured in vitro (Figure 6) and demonstrate that the deficiency of HRI in macrophages leads to the impairment of iron recycling in chronic hemolytic anemia.

Discussion
We showed previously that HRI plays an essential protective role in the anemia of iron deficiency (25), EPP, and β-thalassemia (26).

1R is critical for the growth and maturation of macrophages, as CSF-1R–deficient mice have a considerably decreased number of macrophages (39). Consequently, expression levels of macrophage cell-surface markers F4/80 and CD11b and the core component of the receptor complex for LPS, TLR4 (40), were reduced in *Hri⁻/⁻* compared with *Hri⁺/⁺* macrophages (Figure 3). This is the first demonstration to our knowledge that HRI protein is expressed and functional in nonerythroid cell types.

HRI contributed to 50% of total eIF2α kinase activity in macrophages under in vitro culture conditions (Figures 2 and 5). Importantly, a downstream component of the eIF2αP signaling pathway, Chop, was also expressed at a lower level in *Hri⁻/⁻* mac-

Figure 6
Impaired erythrophagocytosis by *Hri⁻/⁻* BMDMs. (**A**) Phase-contrast images of phagocytosis of aged rbc by control or LPS-treated macrophages. Original magnification, ×200. (**B**) Phagocytosis index (number of rbc/macrophage) and percentage of rbc⁺ macrophages. These quantifications were done by counting the numbers of rbc per macrophage and rbc-containing macrophages in images under a ×200 field. Results are presented as mean ± SEM (*n* = 15–24).

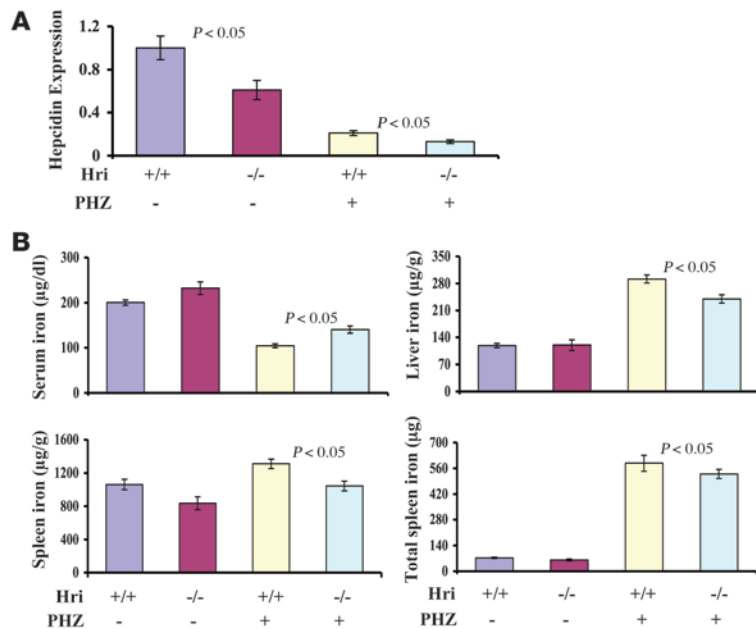rophages. This finding is consistent with the eIF2αP-dependent increase in Chop expression during endoplasmic reticulum stress (34, 35). Recently, it has been shown that LPS-induced inflammatory response in the lung was attenuated in Chop^{–/–} mice due to the suppression of production of caspase-11, which is necessary for the cleavage of pro–IL-1β (41). In addition to heme deficiency, HRI can also be activated by ROS (28). Here, we found that ROS induced by LPS treatment was responsible for the activation of HRI, since LPS-enhanced eIF2αP and Chop expression in *Hri*^{+/+} macrophages was prevented by treatment with the reducing agent β-ME (Figure 5). Thus, the HRI/eIF2αP pathway may be important in the maturation of macrophages and in their response to acute inflammation induced by LPS treatment.

The recognition and sensing of LPS involves a complex orchestration of protein-protein interactions (reviewed in refs. 42, 43). TLR4 is the vital component of the core TLR4/MD2/CD14 LPS-sensing complex; LPS signaling transduction is hampered in TLR4-deficient mice (44). However, other molecules, such as CD11b/CD18 and CD55, are also involved in the LPS sensing and in the subsequent induction of gene expression (reviewed in refs. 45, 46). The reduced expression of TLR4, CD11b, and Chop in *Hri*^{–/–} macrophages may result in the blunted inflammatory response in HRI deficiency (Figures 3 and 5).

Both acute and chronic inflammation result in AI (reviewed in refs. 20, 21). Cytokine production is part of the host immune response to inflammation. Activation of TLR4-induced signaling by LPS leads to a considerable production of inflammatory cytokines such as IL-1, IL-6, and TNF-α (reviewed in refs. 42, 43). Recently, it has been shown that inflammatory cytokines such as IL-1β, IL-6, and IL-1α can increase hepcidin expression (15, 18, 19). This increase in hepcidin is expected to inhibit the recycling of iron from macrophages by targeting ferroportin protein for degradation and thus resulting in iron-restrictive erythropoiesis and anemia. Although inflammatory cytokines (IL-6 and TNF-α) were greatly increased upon LPS treatment, *Hri*^{–/–} mice and macrophages had weakened responses to LPS in producing inflamma-

tory cytokines compared with *Hri*^{+/+} mice (Figures 3 and 4). This weakened IL-1 and IL-6 production may be responsible for the lower hepatic hepcidin mRNA level in *Hri*^{–/–} mice after LPS treatment (Figure 4). Thus, iron egress from macrophages to plasma was more restricted in *Hri*^{+/+} mice than in *Hri*^{–/–} mice upon LPS treatment, as indicated by higher serum iron and lower splenic iron content in *Hri*^{–/–} mice (Figure 4). The molecular mechanism for the decreased expression of hepcidin in HRI deficiency under normal conditions remains to be further investigated. Since *Hri*^{–/–} mice had no detectable anemia (25), defective maturation of *Hri*^{–/–} macrophages may contribute to the lower hepcidin expression through macrophage-derived factor(s) as yet unknown.

The importance of HRI in iron homeostasis is further demonstrated in a mouse model of chronic hemolytic anemia induced by PHZ (Figures 7 and 8). PHZ is widely used to induce hemolysis because it provokes denaturation of oxyhemoglobin, accumulation of Heinz bodies in erythrocytes, and damage of cells (47). The damaged rbc are mostly engulfed by macrophages in the spleen and liver. Recycling of iron from erythrophagocytosis by macrophages plays a critical role in erythropoiesis during chronic hemolytic anemia. Under the condition of mild chronic hemolytic anemia, both *Hri*^{+/+} and *Hri*^{–/–} mice were able to compensate by increasing erythropoiesis and iron absorption. No significant reduction in hemoglobin was observed in PHZ-treated mice. However, PHZ-treated *Hri*^{–/–} mice exhibited impaired erythrophagocytosis by splenic and hepatic macrophages (Figure 8). The reduction in the increase of liver and spleen iron concentrations in *Hri*^{–/–} mice upon PHZ treatment is consistent with the decreased erythrophagocytosis by *Hri*^{–/–} macrophages. These findings provide evidence of the role of HRI in macrophages to recycle iron for erythropoiesis. In this regard, HRI also coordinates the supply of iron for hemoglobin synthesis in erythroid cells by recycling it from senescent rbc under the stress conditions of hemolytic anemia.

Macrophages are essential for definitive erythropoiesis (48, 49). Erythroblastic islands consisting of a central macrophage with a number of erythroblasts surrounding its plasma membrane
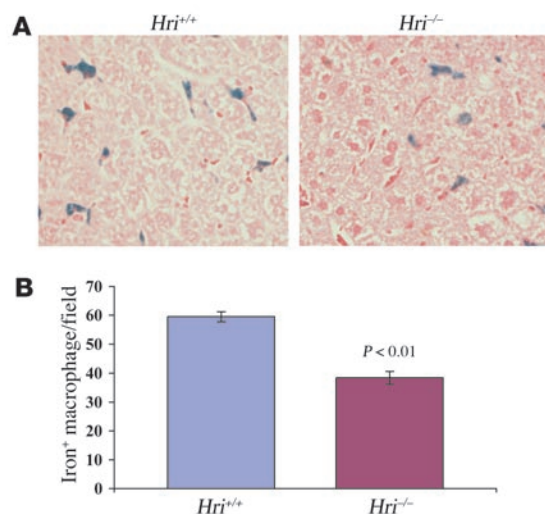
Figure 8
Impaired erythrophagocytosis by Kupffer cells in *Hri*^{−/−} mice during chronic hemolytic anemia induced by PHZ. (**A**) Iron staining of liver tissue sections of *Hri*^{+/+} and *Hri*^{−/−} mice after PHZ treatment. (**B**) Numbers of iron-laden macrophages/field. The values represent the average number of iron-laden macrophages under a ×200 field (*n* = 10).

provide special microenvironments for the proliferation, differentiation, and enucleation of erythroblasts (reviewed in ref. 50). Macrophages are proposed to provide cytokines for erythroblast proliferation as well as to iron for hemoglobin synthesis. Therefore, expression of HRI in macrophages in addition to erythroid cells may serve to coordinate the proliferation and terminal differentiation of erythroblasts.

In summary, our present studies of inflammatory response and chronic hemolytic anemia in *Hri*^{−/−} mice reveal a novel function of HRI in macrophages.

Methods

Mouse strains, breeding, and genotyping. All mouse production and experimentation were approved by the Committee on Animal Care at Massachusetts Institute of Technology. *Hri*^{−/−} mice on an inbred B6.129 mixed genetic background were generated in our laboratory as described previously (25). Genotyping was performed by PCR of tail DNA. PCR reactions of the Hri gene were performed as described previously (25).

Hematological analysis and non-heme iron assays. Blood, liver, and spleen samples were collected from 4-month-old mice. The hematological analyses of peripheral blood and reticulocyte counts were performed as described previously (25, 51). Non-heme tissue iron was assayed as previously described (28, 52).

qRT-PCR. Total RNAs were isolated from the liver and macrophages using Total RNA Isolation kit (Promega). Quantitative measurements of gene expression were carried out with DNA Engine Opticon 2 (MJ Research) equipped with Opticon Monitor 2 software. eIF2α was used as an internal control. Primer sequences for RT-PCR were hepcidin: forward 5′-CTGAGCAGCACCACCTATCTC-3′, reverse 5′-TGGCTCTAGGCTAT-GTTTTGC-3′; Hri: forward 5′-AGCAGTTCGTCCATTGTCTTTG, reverse CCGTGTAGCTCACCAGGTT; eIF2α: forward GGAAGCAATCAAATG-TGAGGA-CA, reverse: GCACCGTATCCAGGTCTCTTG.

Cell culture of BMDMs and LPS treatment. BMDMs were isolated and cultured as previously described (53). Briefly, bone marrow cells were

flushed from the femur and tibia of 6- to 8-week-old male mice, washed twice with PBS plus 2% FBS, and then cultured in DMEM with high glucose, glutamine, 15% heat-inactivated FBS, 25 ng/ml rmCSF-1 (Pepro-Tech), nonessential amino acids (Cambrex), penicillin/streptomycin (Invitrogen), and 55 nM β-ME (Sigma-Aldrich) at 37°C, 5% CO_2. Three days after seeding, cells were washed twice with PBS, and the medium was changed every day until day 7.

BMDMs at day 7 were treated with 1,000 ng/ml of LPS, and cell culture media were collected for ELISA at 0.5, 1, 3, and 6 hours. Cells were then collected for RNA extractions and cell lysate preparations for Western blot analysis. For the activation of macrophages in erythrophagocytosis, BMDMs were treated with 100 ng/ml of LPS overnight.

In vivo LPS treatment and ELISA. Four-month-old male mice were treated with 1 intraperitoneal injection (1 μg/g body weight) of LPS (serotype O111:B4; Sigma-Aldrich) in pyrogen-free PBS. Six or 24 hours later, sera were collected for measurements of cytokines and non-heme iron. At the same time, spleen and liver samples were also collected for the non-heme tissue iron analysis and RNA extractions. Cytokines in the sera and culture media of BMDMs were measured according to the manufacturer's instructions (TNF-α, IL-1β, and IL-6; eBioscience).

Immunofluorescence microscopy. Immunofluorescence study was done according to the standard procedures. BMDMs were cultured on coverslips as described above and were fixed in 4% paraformaldehyde for 15 minutes at 37°C. After washing 3 times with PBS, cells were permeabilized with 0.1% Triton X-100 in PBS for 10 minutes at room temperature. Cells were blocked for 2 hours with PBS plus 5% normal goat serum and 1% BSA. Cells were incubated overnight at 4°C with 1:500 anti-HRI IgG and 1:10 anti-CD11b (Mac-1) antibody (BD Biosciences − Pharmingen). Cells were then washed 5 times with PBS followed by incubation for 90 min with the anti-rabbit (for HRI) or anti-rat (for Mac-1) IgG secondary antibody conjugated with Alexa Fluor 488 or Alexa Fluor 633 (Molecular Probes; Invitrogen). After washing with PBS, coverslips were air dried and then mounted with anti-fading mounting reagent and examined by an LSM 410 inverted laser scan microscope (LSM Technologies Inc.).

Flow cytometry. Expression of CD11b, F4/80, and TLR4 in bone marrow cells and BMDMs were examined by flow cytometry. Cultured BMDMs were detached from the culture dishes on days 3 and 6 by treatment with 5 mM EDTA for 15 minutes. Both bone marrow cells and BMDMs were washed twice with PBS and then stained with allophycocyanin-conjugated rat anti-mouse CD11b monoclonal antibody (BD Biosciences), FITC-conjugated rat anti-mouse F4/80 monoclonal antibody (eBioscience), or PE-conjugated rat anti-mouse TLR4 monoclonal antibody (Santa Cruz Biotechnology Inc.) for 30 minutes on ice. After washing 3 times with PBS, cells were analyzed by flow cytometry as described previously (25).

The level of cellular ROS was examined by FACS analysis using cells treated with 5 μM of DCF (Molecular Probes; Invitrogen) at 37°C as previously described (54). Briefly, cells were incubated with DCF in DMEM medium for 30 minutes and then treated with LPS (1,000 ng/ml) with or without β-ME (14.3 μM) for 6 hours. Cells were then collected for flow cytometry and Western blot analyses.

Western blot analysis. Protein extracts were prepared from macrophages as previously described (25). Protein extracts (20 μg) were separated by 7.5% and 10% (for HRI) and 12% (for other proteins) SDS-PAGE and processed for Western blot analyses as described previously (25). Antibodies used were the affinity-purified anti-mouse N-terminal HRI antibody (1:1,000), anti-eIF2α antibody (1:1,000; BioSource), anti-eIF2αP antibody (1:1,000; BioSource), anti–CSF-1R (1:500; Santa Cruz Biotechnology Inc.), or anti-Chop (1:500; Santa Cruz Biotechnology Inc.). The intensities of western signals in autoradiograms were quantitated by Alpha Ease FC software (Alpha Innotech).

Erythrophagocytosis. Senescence of rbc was induced by increasing intracellular calcium concentration as previously described (55). After washing twice with PBS, rbc were resuspended in 10 mM HEPES, 140 mM NaCl, BSA 0.1%, pH 7.4, at a concentration of 1×10^8 rbc/ml. $CaCl_2$ and Ca^{+2} ionophore A23187 (Calbiochem) were added to rbc suspension at final concentrations of 2.5 mM and 0.5 μM, respectively, and the samples were then incubated at 30°C for 16 hours. Untreated rbc were kept at 4°C. Both treated and untreated rbc were washed twice with PBS and resuspended in PBS. Treated aged or untreated rbc were incubated with BMDMs (3×10^7 rbc/well in 24-well plates). Noningested rbc were lysed with an rbc lysis buffer (eBioscience). Samples were visualized by phase-contrast microscopy, and macrophages with ingested rbc as well as rbc per macrophage were quantified.

Chronic hemolytic anemia mouse model. PHZ (Sigma-Aldrich), freshly prepared in PBS, was injected intraperitoneally into mice to induce chronic hemolytic anemia as previously described (17). PHZ was given twice a week at a low dose (30 mg/kg) for 4 weeks. Mice were sacrificed at 64 hours after the final injection of PHZ, and blood, spleen, and liver samples were collected for complete blood count, iron, and hepcidin analyses.

Pathological analysis. Tissues were fixed in formalin and then processed for paraffin embedding and sectioning using standard procedures by the MIT Division of Comparative Medicine. Sections were stained with H&E. Liver and spleen non-heme iron were stained with Prussian blue as described previously (54).

Statistics. Statistical analyses among the various groups were performed by 2-tailed Student *t* test, with a *P* value of less than 0.05 considered statistically significant.

Address correspondence to: Jane-Jane Chen, E25-545, Massachusetts Institute of Technology, 77 Massachusetts Avenue, Cambridge, Massachusetts 02139, USA. Phone: (617) 253-9674; Fax: (617) 253-3459; E-mail: j-jchen@mit.edu.

1. Ganz, T., and Nemeth, E. 2006. Regulation of iron acquisition and iron distribution in mammals. *Biochim. Biophys. Acta.* **1763**:690–699.
2. Andrews, N.C., and Schmidt, P.J. 2007. Iron homeostasis. *Annu. Rev. Physiol.* **69**:69–85.
3. Stoltzfus, R.J. 2003. Iron deficiency: global prevalence and consequences. *Food. Nutr. Bull.* **24**:S99–S103.
4. Knutson, M.D., Walter, P.B., Ames, B.N., and Viteri, F.E. 2000. Both iron deficiency and daily iron supplements increase lipid peroxidation in rats. *J. Nutr.* **130**:621–628.
5. Camaschella, C. 2005. Understanding iron homeostasis through genetic analysis of hemochromatosis and related disorders. *Blood.* **106**:3710–3717.
6. Nicolas, G., et al. 2001. Lack of hepcidin gene expression and severe tissue iron overload in upstream stimulatory factor 2 (USF2) knockout mice. *Proc. Natl. Acad. Sci. U. S. A.* **98**:8780–8785.
7. Lesbordes-Brion, J.C., et al. 2006. Targeted disruption of the hepcidin 1 gene results in severe hemochromatosis. *Blood.* **108**:1402–1405.
8. Roetto, A., et al. 2003. Mutant antimicrobial peptide hepcidin is associated with severe juvenile hemochromatosis. *Nat. Genet.* **33**:21–22.
9. Nicolas, G., et al. 2002. Severe iron deficiency anemia in transgenic mice expressing liver hepcidin. *Proc. Natl. Acad. Sci. U S A.* **99**:4596–601.
10. Nemeth, E., et al. 2004. Hepcidin regulates cellular iron efflux by binding to ferroportin and inducing its internalization. *Science.* **306**:2090–2093.
11. Pigeon, C., et al. 2001. A new mouse liver-specific gene, encoding a protein homologous to human antimicrobial peptide hepcidin, is overexpressed during iron overload. *J. Biol. Chem.* **276**:7811–7819.
12. Nicolas, G., et al. 2002. The gene encoding the iron regulatory peptide hepcidin is regulated by anemia, hypoxia, and inflammation. *J. Clin. Invest.* **110**:1037–1044. doi:10.1172/JCI200215686.
13. Nemeth, E., et al. 2003. Hepcidin, a putative mediator of anemia of inflammation, is a type II acute-phase protein. *Blood.* **101**:2461–2463.
14. Nemeth, E., et al. 2004. IL-6 mediates hypoferremia of inflammation by inducing the synthesis of the iron regulatory hormone hepcidin. *J. Clin. Invest.* **113**:1271–1276. doi:10.1172/JCI200420945.
15. Lee, P., Peng, H., Gelbart, T., Wang, L., and Beutler, E. 2005. Regulation of hepcidin transcription by interleukin-1 and interleukin-6. *Proc. Natl. Acad. Sci. U. S. A.* **102**:1906–1910.
16. Pak, M., Lopez, M.A., Gabayan, V., Ganz, T., and Rivera, S. 2006. Suppression of hepcidin during anemia requires erythropoietic activity. *Blood.* **108**:3730–3735.
17. Vokurka, M., Krijt, J., Sulc, K., and Necas, E. 2006. Hepcidin mRNA levels in mouse liver respond to inhibition of erythropoiesis. *Physiol. Res.* **55**:667–674.
18. Wrighting, D.M., and Andrews, N.C. 2006. Interleukin-6 induces hepcidin expression through STAT3. *Blood.* **108**:3204–3209.
19. Verga Falzacappa, M.V., et al. 2007. STAT3 mediates hepatic hepcidin expression and its inflammatory stimulation. *Blood.* **109**:353–358.
20. Ganz, T. 2003. Hepcidin, a key regulator of iron metabolism and mediator of anemia of inflammation. *Blood.* **102**:783–788.
21. Roy, C.N., and Andrews, N.C. 2005. Anemia of inflammation: the hepcidin link. *Curr. Opin. Hematol.* **12**:107–111.
22. Cartwright, G.E. 1966. The anemia of chronic disorders. *Semin. Hematol.* **3**:351–375.
23. Weinstein, D.A., et al. 2002. Inappropriate expression of hepcidin is associated with iron refractory anemia: implications for the anemia of chronic disease. *Blood.* **100**:3776–3781.
24. Rivera, S., et al. 2005. Hepcidin excess induces the sequestration of iron and exacerbates tumor-associated anemia. *Blood.* **105**:1797–1802.
25. Han, A.P., et al. 2001. Heme-regulated eIF2alpha kinase (HRI) is required for translational regulation and survival of erythroid precursors in iron deficiency. *EMBO J.* **20**:6909–6918.
26. Han, A.P., Fleming, M.D., and Chen, J.J. 2005. Heme-regulated eIF2α kinase modifies the phenotypic severity of murine models of erythropoietic protoporphyria and β-thalassemia. *J. Clin. Invest.* **115**:1562–1570. doi:10.1172/JCI24141.
27. Chen, J.J. 2007. Regulation of protein synthesis by the heme-regulated eIF2{alpha} kinase: relevance to anemias. *Blood.* **109**:2693–2699.
28. Lu, L., Han, A.P., and Chen, J.J. 2001. Translation initiation control by heme-regulated eukaryotic initiation factor 2alpha kinase in erythroid cells under cytoplasmic stresses. *Mol. Cell. Biol.* **21**:7971–7980.
29. Crosby, J.S., Lee, K., London, I.M., and Chen, J.J. 1994. Erythroid expression of the heme-regulated eIF-2 alpha kinase. *Mol. Cell. Biol.* **14**:3906–3914.
30. Chitu, V., and Stanley, E.R. 2006. Colony-stimulating factor-1 in immunity and inflammation. *Curr. Opin. Immunol.* **18**:39–48.
31. Roy, C.N., et al. 2004. An Hfe-dependent pathway mediates hyposideremia in response to lipopolysaccharide-induced inflammation in mice. *Nat. Genet.* **36**:481–485.
32. Hsu, L.C., et al. 2004. The protein kinase PKR is required for macrophage apoptosis after activation of Toll-like receptor 4. *Nature.* **428**:341–345.
33. Yamada, H., et al. 2006. LPS-induced ROS generation and changes in glutathione level and their relation to the maturation of human monocyte-derived dendritic cells. *Life Sci.* **78**:926–933.
34. Harding, H.P., et al. 2000. Regulated translation initiation controls stress-induced gene expression in mammalian cells. *Mol. Cell.* **6**:1099–1108.
35. Scheuner, D., et al. 2001. Translational control is required for the unfolded protein response and in vivo glucose homeostasis. *Mol. Cell.* **7**:1165–1176.
36. Ferrali, M., et al. 1997. Release of free, redox-active iron in the liver and DNA oxidative damage following phenylhydrazine intoxication. *Biochem. Pharmacol.* **53**:1743–1751.
37. Frazer, D.M., et al. 2004. Delayed hepcidin response explains the lag period in iron absorption following a stimulus to increase erythropoiesis. *Gut.* **53**:1509–1155.
38. Stout, R.D., and Suttles, J. 2005. Immunosenescence and macrophage functional plasticity: dysregulation of macrophage function by age-associated microenvironmental changes. *Immunol. Rev.* **205**:60–71.
39. Dai, X.M., et al. 2002. Targeted disruption of the mouse colony-stimulating factor 1 receptor gene results in osteopetrosis, mononuclear phagocyte deficiency, increased primitive progenitor cell frequencies, and reproductive defects. *Blood.* **99**:111–120.
40. Akashi, S., et al. 2000. Cutting edge: cell surface expression and lipopolysaccharide signaling via the toll-like receptor 4–MD-2 complex on mouse peritoneal macrophages. *J. Immunol.* **164**:3471–3475.
41. Endo, M., Mori, M., Akira, S., and Gotoh, T. 2006. C/EBP homologous protein (CHOP) is crucial for the induction of caspase-11 and the pathogenesis of lipopolysaccharide-induced inflammation. *J. Immunol.* **176**:6245–6253.
42. Aderem, A., and Ulevitch, R.J. 2000. Toll-like receptors in the induction of the innate immune response. *Nature.* **406**:782–787.
43. Miller, S.I., Ernst, R.K., and Bader, M.W. 2005. LPS, TLR4, and infectious disease diversity. *Nat. Rev. Microbiol.* **3**:36–46.
44. Poltorak, A., et al. 1998. Defective LPS signaling in

C3H/HeJ and C57BL/10ScCr mice: mutations in Tlr4 gene. *Science.* **282**:2085–2088.

45. Dobrovolskaia, M.A., and Vogel, S.N. 2002. Toll receptors, CD14, and macrophage activation and deactivation by LPS. *Microbes Infect.* **4**:903–914.

46. Triantafilou, M., and Triantafilou, K. 2005. The dynamics of LPS recognition: complex orchestration of multiple receptors. *J. Endotoxin Res.* **11**:5–11.

47. Itano, H.A., Hirota, K., and Hosokawa, K. 1975. Mechanism of induction of haemolytic anaemia by phenylhydrazine. *Nature.* **256**:665–667.

48. Kawane, K., et al. 2001. Requirement of DNase II for definitive erythropoiesis in the mouse fetal liver. *Science.* **292**:1546–1549.

49. Krieser, R. J., et al. 2002. Deoxyribonuclease IIalpha is required during the phagocytic phase of apoptosis and its loss causes perinatal lethality. *Cell Death Differ.* **9**:956–962.

50. Chasis, J. A. 2006. Erythroblastic islands: specialized microenvironmental niches for erythropoiesis. *Curr. Opin. Hematol.* **13**:137–141.

51. Lee, L.G., Chen, C.H., and Chiu, L.A. 1986. Thiazole orange: a new dye for reticulocyte analysis. *Cytometry.* **7**:508–517.

52. Torrance, J.D., and Bothwell, T.H. 1980. Tissue iron stores. In *Methods in hematology.* J.D. Cook, editor. Churchill Livingstone Press. New York, New York, USA. 104–109.

53. Delaby, C., Pilard, N., Goncalves, A.S., Beaumont, C., and Canonne-Hergaux, F. 2005. Presence of the iron exporter ferroportin at the plasma membrane of macrophages is enhanced by iron loading and down–regulated by hepcidin. *Blood.* **106**:3979–3984.

54. Harding, H.P., et al. 2003. An integrated stress response regulates amino acid metabolism and resistance to oxidative stress. *Mol. Cell.* **11**:619–633.

55. Delaby, C., et al. 2005. A physiological model to study iron recycling in macrophages. *Exp. Cell Res.* **310**:43–53.